BHR Group
EXPERTS IN FLUID ENGINEERING

Large scale experiments on high-rate three-phase low liquid loading flows

Jørn Kjølaas, Tor Erling Unander, Heiner Schümann, Marita Wolden, SINTEF, Norway
Henning Holm, Equinor, Norway

ABSTRACT

A comprehensive three-phase flow campaign, funded by Equinor as part of the Tanzania gas field development project [1] [2] [3], was carried out in the SINTEF Large Scale Loop at Tiller in 2017-2018. The experiments were conducted in a 94 meter long 8" pipe, with 2.5° inclination at 60 bar nominal system pressure, using nitrogen, Exxsol D60 and water with and without glycerol. The motivation for performing this study was to support model development targeted towards reducing prediction uncertainty for high-rate low liquid loading conditions. Specifically, the experiments were conducted at conditions that to a certain extent matched those expected during plateau production for the subsea gas development in Block 2 offshore Tanzania. One of the key concerns was that the presence of oil, water and MEG increases the frictional pressure drop more than current multiphase models predict.

The focus of the work was on gas dominated three-phase flows, with low liquid rates (USL=0.0001-0.1 m/s), and mainly high gas rates (USG=4-14 m/s). The effect of the water viscosity was investigated by mixing glycerol (70-74%) with the water, and conducting experiments at different temperatures, yielding water viscosities in the range 14-42 cP. The aim of the experimental campaign was to produce experimental data relevant for modelling two- and three-phase low liquid loading flows at high gas rates. Earlier experiments [4] had revealed that the pressure drop was significantly higher in three-phase flows compared to two-phase flows, and the current experiments were conducted to investigate this phenomenon more thoroughly.

In this paper we provide an overview of the experimental campaign, and we show some of the key results. Some of the main findings from the experiments were:

- The pressure drop depends significantly on the water cut. In general, the pressure drop increases with water cut, reaching a maximum value at around WC=80%, after which the pressure drop decreases again.
- For three-phase experiments with tap water, the maximum pressure drop was typically 20-40% higher than for two-phase gas-oil, while with the water/glycerol mixture, the maximum pressure drop could be up to 80-100% higher than for the gas-oil system.
- For high water cuts, the frictional pressure drop increases with increasing water viscosity, while for low water cuts, the frictional pressure drop is independent of the water properties.

1 INTRODUCTION

Low liquid loading generally refers to flow conditions where the superficial liquid velocity is small compared to the superficial gas velocity. This is a typical scenario for wet gas lines, where the reservoir produces mostly gas, but where changes in the pressure and temperature along the pipe causes condensation of water and hydrocarbons, so that the liquid rate increases with the distance from the well.

At high gas flow rates, the main modelling challenge is to predict the pressure drop accurately, which in the presence of even tiny amounts of liquid can be difficult. Indeed, Kjølaas et al. [4] showed that seemingly insignificant liquid fractions can increase the pressure drop significantly compared to single phase gas systems, and in three-phase scenarios, the pressure drop can in addition depend significantly on the water cut. These observations were at the time somewhat unexpected and were not well accounted for by multiphase models [5].

It was argued at the time [4] [5] that one of the main mechanisms responsible for the unexpectedly high pressure drop in these conditions was that the droplets entrained from the liquid at the bottom of the pipe deposited on the wall, forming a thin film with a roughness that far exceeded that of the dry wall. This rough film subsequently increases the shear stress experienced by the gas, thus leading to higher pressure drop. With this hypothesis, the observed three-phase effects could be at least partially understood by postulating that the roughness of the film on the wall increased with the effective viscosity of the liquid. Indeed, if the oil and water are fully mixed, the effective liquid viscosity typically increases with the water fraction for low water fractions, and then reaches a maximum value before decreasing again as the water fraction approaches unity [6]. The exact nature of this behaviour can however not be determined a priori from the thermodynamic properties of the pure phases. Instead, one needs to conduct special experiments to find such relations for a given fluid system, which is what we did here. This is briefly described in section 3, and a more thorough description of these experiments is presented by Schümann [7].

The discrepancies between model predictions and measured pressure drop in high-rate low liquid loading flows raised some concerns for the Tanzania gas development project. In this field, the produced fluids will be transported on the sea floor around 100 km to the receiving onshore facilities. An average pressure drop error of 10-20 Pa/m for this particular flowline would yield an accumulated error of 10-20 bar in total pressure drop, which could have serious consequences for the capacity of the system. Thus, to mitigate this prediction problem, the experimental campaign described here was launched with the aim of using the data to improve current multiphase models, thereby reducing the uncertainty in the pressure drop predictions.

In the available literature, we did find some experimental studies of high-rate three-phase flows in low liquid loading conditions [8] [9] [10] [11], but just about all those studies were conducted at near-atmospheric pressure. Although low-pressure systems may be academically interesting, they are very far from the typical conditions in wet gas transport lines, so it is risky to rely heavily on such data in the development of models aimed at industrial applications. In particular, the significant three-phase effects that we had observed at high pressure did not appear to prevail in most of these low pressure experiments. Consequently, it was concluded that there was a definite need for high-rate low liquid loading data at high pressure in order to progress on this matter. A new experimental campaign was therefore initiated in order to further investigate these phenomena, and to hopefully gain some additional insight into the physical mechanisms responsible for the observed behaviour.

To summarize, this paper presents an experimental study of low liquid loading in high-rate low liquid loading three-phase flows with special focus on the effect of water cut on the pressure drop. The aim of this work was to obtain relevant data covering a wide range of conditions and fluid properties, for the purpose of improving the understanding of the complex physics at work at these conditions, and subsequently improve the modelling of multiphase flows.

2 EXPERIMENTAL SETUP

The experiments were conducted at the SINTEF Multiphase Flow Laboratory. The Large Scale Loop Facility was used and adapted with a 94 meter long 8"pipe, with an inclination angle of 2.5°. A photograph of the experimental setup is shown in Figure 1. For the experiments, nitrogen was used as the gas phase and Exxsol D60 as oil phase. The nominal pressure was 60 bara, yielding a gas density of 67 kg/m^3. For the aqueous phase, we used regular tap water with NaOH for corrosion protection, with and without glycerol. The purpose of adding glycerol was to increase the viscosity of the aqueous phase, emulating MEG injection. In the experiments with glycerol, the volumetric concentration was 70-74%. The glycerol experiments were conducted at temperatures of 23°C and 45°C yielding viscosities of about 42 and 14 cP, respectively, while the experiments without glycerol were conducted at 30°C. When changing the temperature, we also adjusted the pressure such that the gas density was kept the same in all the experiments.

After the 8" experiments were completed, a similar set of experiments was conducted in a 12" pipe in order to investigate the effect of the pipe diameter. The trends observed for that data set were consistent with the observations shown in this paper. However, for the sake of brevity, we only include the results from the 8" experiments here.

Figure 1: Photograph of the experimental setup.

The main instrumentation on the test section included five narrow-beam gamma densitometers for liquid height measurements, and five DP-cells attached between the test section and a common reference line to obtain pressure gradients at various positions along the pipe (12.2, 27.1, 41.3, 64.3, 77.5 and 90.7 meters from the start). A schematic illustration of the setup is shown in Figure 2.

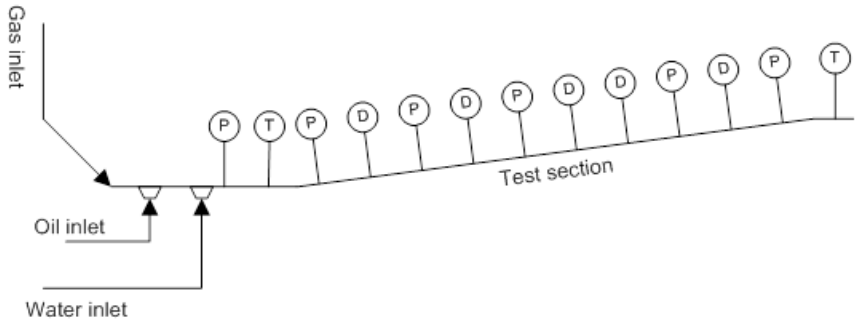

Figure 2: Schematic illustration of the experimental setup. The test section was equipped with DP-cells (labelled P), gamma densitometers (labelled D) and temperature transmitters (labelled T).

The gas and liquid flow rates were measured using Micro Motion Coriolis meters [12]. For each of the liquid phases, four Coriolis meters were installed to cover the wide range of flow rates applied in this campaign. The pressure drop was measured using five DP-cells attached between the test section and a common reference line to obtain pressure gradients at various positions along the pipe. The liquid height was measured with high temporal resolution using five vertically oriented narrow-beam gamma densitometers. In addition, two gamma-based scanning densitometers were installed on the test section to measure the time-averaged vertical density profiles. The most important measurement uncertainties are listed in Table 1.

Table 1: Measurement uncertainties (expressed as one standard deviation).

Quantity	Uncertainty		Quantity	Uncertainty
Liquid density	1.4 kg/m³		*USG*	1.2 %
Gas density	0.1 kg/m³		Liquid holdup	0.01
USL	0.4 %		Pressure drop	3-5 Pa/m

The gas properties were calculated from the measured pressure and temperature using reference values obtained from NIST [13]. The liquid density was measured online by the Coriolis meters, and the liquid viscosities were measured offline by pumping the liquid samples through a pressurized coiled steel capillary pipe (length L = 250 cm, inner radius r = 400 μm, coil radius R = 3.0 cm), and measuring the pressure loss. The surface tension was measured by the pendant-drop method inside a cylindrical pressurized cell. The thermodynamic properties of the different phases are summarized in Table 2.

Table 2: Fluid properties at 60 bara

Density (kg/m^3)	Nitrogen @ 30°C	69.4
	Exxsol D60 @ 30°C	784
	Water @ 30°C	998.5
	Water+glycerol @ 23°C	1 197
	Water+glycerol @ 45°C	1 181
Viscosity (mPa s)	Nitrogen @ 30°C	0.018
	Exxsol D60 @ 30°C	1.3
	Water @ 30°C	0.8
	Water+glycerol @ 23°C	42
	Water+glycerol @ 45°C	14
Surface tension (mN/m)	Exxsol D60/Nitrogen @ 30°C	19
	Water/Nitrogen @ 30°C	64
	Water+glycerol/Nitrogen @ 23°C	52
	Water+glycerol/Nitrogen @ 45°C	52

The rheological behaviour of the oil/water system for these oil-water systems were investigated using a small-scale low-pressure setup. This setup and prevailing results are described in the next section.

3 RHEOLOGY OF THE OIL-WATER SYSTEMS

As mentioned before the formation of oil-water dispersions will cause an increase in the apparent viscosity of the liquid mixture. In order to correctly predict the pressure drop of the system, the apparent viscosity of the dispersions formed has to be provided in some way.

The rheological properties of the fluid systems used in the campaign were tested in a small scale flow loop setup functioning as a pipe rheometer. Here, dispersions were created by a mixing valve and continued to flow through a short pipe section of 2 m length and 8 mm in diameter. The loop was operated at approximately 1 m/s mixture velocity. A pressure drop over the mixing valve of approximately 0.5 bar combined with the short pipe section secured dispersed flow throughout the test section. The pressure drop over the test section was used to calculate the friction factor. The apparent viscosity of the dispersed system was then back-calculated from the friction factor, assuming either laminar or turbulent flow. In the case of turbulent flow, the Håland friction factor model [14] was used.

The measured viscosities are shown in Figure 3 (top graph). Note, only fully laminar or turbulent points are shown, neglecting measurements in the transition region. As expected, apparent viscosities increase towards the phase inversion point indicated by the peak measurements. With increasing viscosity of the water phase the inversion point shifts towards higher water cut. The measured pressure drop normalized with the single phase

oil pressure drop is shown in the bottom graph and compared with predictions obtained using LedaFlow forcing fully mixed oil-water flow combined with the Brinkman emulsion model [15]. Here, we have assumed that the inversion point occurs at the point where the effective viscosity of the oil-continuous mixture and the water-continuous mixture are the same. The predictions match the measurements relatively well in the case of water-glycerol. For regular water the peak values close to the inversion point are however somewhat underpredicted.

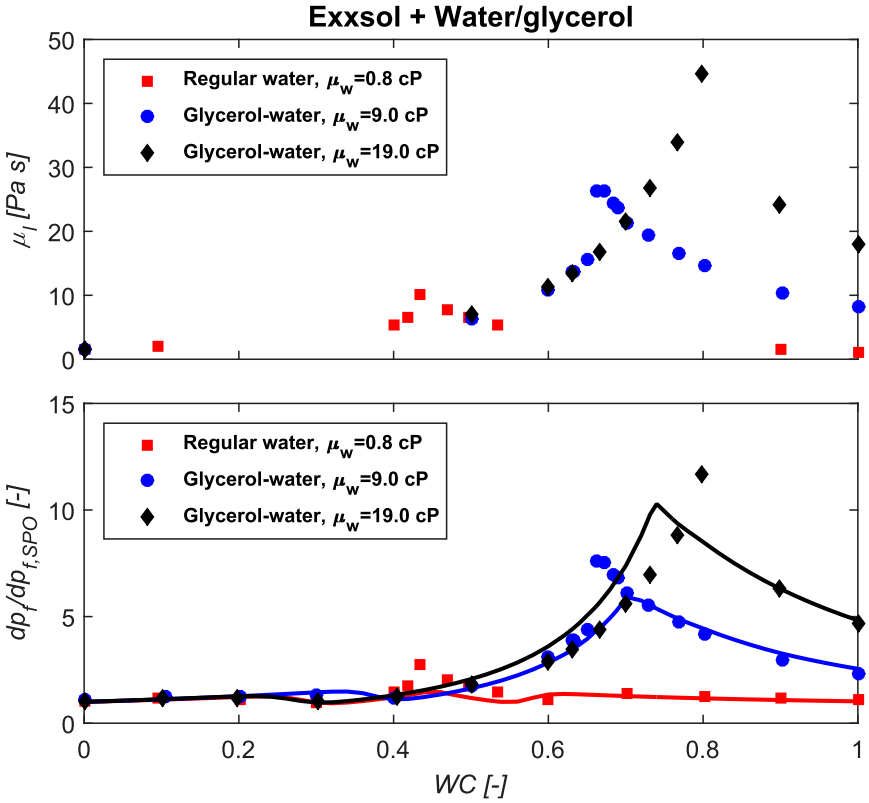

Figure 3: Measured viscosity (top) and pressure drop normalized with the single phase oil pressure drop (bottom) for the small-scale oil-water experiments. The lines are predictions obtained using LedaFlow forcing fully mixed oil-water flow combined with the Brinkman emulsion model.

For more details on these experiments and associated analyses, we refer to the work reported by Schümann et al. [7].

4 EXPERIMENTAL RESULTS

In this section, the main results obtained in the experiments conducted in low liquid loading conditions with high *USG* are summarized. In the graphs below, the flow resistance is shown in terms of the "normalized pressure drop". The normalized pressure drop is defined as the frictional pressure drop divided by the frictional pressure drop in single phase gas flow at the same gas rate. The frictional pressure drop is calculated by subtracting the gravitational pressure drop from the total pressure drop:

$$\left|\frac{dp}{dx}\right|_{fric} = -\frac{dp}{dx} - \rho_{mix} \cdot g \sin\phi \qquad (1)$$

Here, ρ_{mix} is the volumetric mixture density, g is the gravity acceleration, and ϕ is the pipe angle. The mixture density was measured using the traversing gamma densitometers.

The experiments were executed to establish trends with respect to the key parameters:

1) *USG* sweeps, varying *USG*, keeping all other parameters fixed.
2) *USL* sweeps, varying *USL*, keeping all other parameters fixed.
3) Water cut sweeps, varying the water cut, keeping all other parameters fixed.

Examples of the three different types of experiment series are shown in Figure 4:

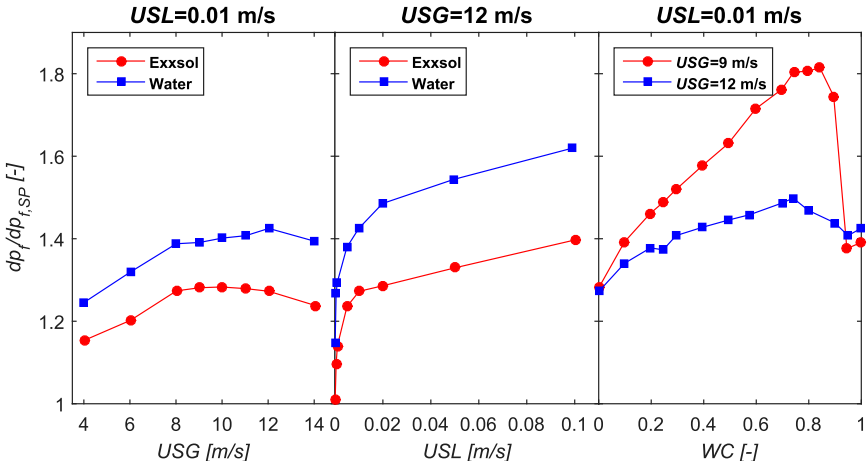

Figure 4: Examples of experiment results in terms of normalized pressure drop. Left: *USG*-sweeps, Middle: *USL*-sweeps, Right: Water cut sweeps.

During the campaign, the results were continuously processed and plotted on an aggregated level (trends and comparison with previous data points), and those results were distributed on email to all people involved as soon as a new data point had been recorded. This online quality assurance system allowed for rapid identification of experimental errors and deviations and was as a key success factor for the project.

4.1 Two-phase gas-liquid flow

Figure 5 shows the normalized pressure drop and liquid holdup plotted against the superficial gas velocity *USG* for two different superficial liquid velocities (*USL*=0.01 m/s

and *USL*=0.1 m/s). The dashed lines in the graphs represent the liquid holdup measured using the traversing gamma densitometers. For the experiments with gas and water, the pressure drop increases with increasing viscosity. Exxsol on the other hand, which has a higher viscosity than water, produces a lower pressure drop than water. We may however note that Exxsol has lower surface tension than water, so these results indicate that the frictional pressure drop increases with both the liquid viscosity and the gas-liquid surface tension. It is also possible that differences in the wetting properties of oil and water towards the steel wall has an impact. The liquid holdup decreases with increasing *USG*, as expected. We also observe that the liquid holdup increases with the liquid viscosity for the experiments with water.

For the lowest liquid rate (*USL*=0.01 m/s), the normalized pressure drop increases with increasing *USG* for moderate gas rates. The normalized pressure drop then reaches a maximum value, after which it decreases with increasing *USG*. A qualitative explanation of this trend in the pressure drop is that the initial increase in the normalized pressure drop is due to a gradual build-up of a liquid film on the wall in the gas zone as the gas rate increases. As explained in the introduction, this wall film leads to a high apparent wall roughness seen by the gas, leading to increased flow resistance. This wall film is a direct result of droplets depositing on the wall, so the extent of the wall film increases as the "height" of the droplet field increases (and the height of the droplet field increases with *USG*). At a certain gas rate, the entire wall in the gas zone is covered by this wall film, and the average "wall" roughness in the gas zone reaches its maximum value. Increasing *USG* beyond this point obviously cannot increase the extent of the wall film. Instead, the wall film presumably becomes thinner and less rough as *USG* is increased, which explains why the normalized pressure drop starts to decrease. A more detailed description of this process can be found in [16].

For *USL*=0.1 m/s, we do not see the same trend. Here, the normalized pressure drop is quite high for low *USG*, and it decreases more or less monotonously with increasing *USG*. It could simply be that the effects observed for *USL*=0.01 m/s also prevail here, but they are perhaps obscured by other phenomena related to the thick film at the bottom of the pipe.

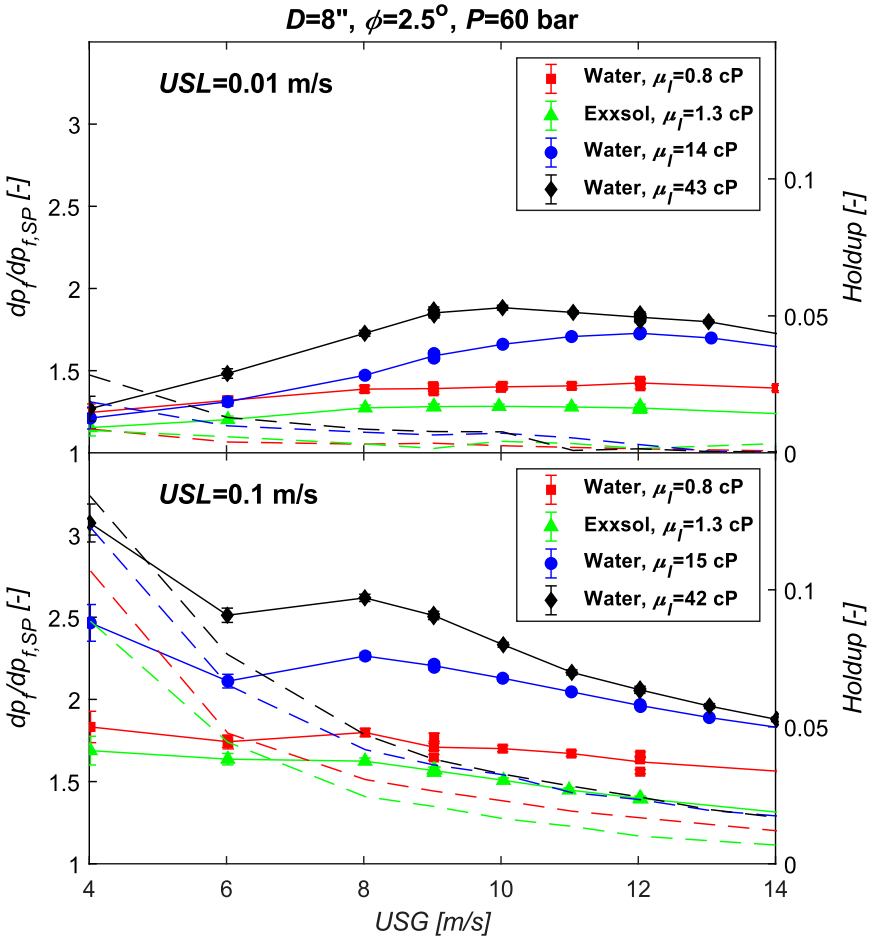

Figure 5: Normalized pressure drop (markers and solid lines) and holdup (dashed lines) plotted against *USG* for *USL*=0.01 and 0.1 m/s for the four different liquids.

Figure 6 shows the normalized pressure drop and holdup plotted against the superficial liquid velocity *USL* for two different superficial gas velocities (*USG*=9 m/s and *USL*=12 m/s). Because of the wide range of liquid rates, the horizontal axis is logarithmic in these graphs. We observe that both the normalized pressure drop and holdup always increases with increasing *USL*. We also observe that the trends we found with respect to the liquid properties in Figure 5 hold true here as well.

For very low *USL* (10^{-4} m/s), the pressure drop in the gas-oil system is approximately equal to the pressure drop in single phase gas, while for the associated gas-water systems, the pressure drop is typically 10-30% higher, depending on the gas flow rate and water viscosity. These experiments were conducted by starting with a dry pipe, so this "jump" in pressure drop going from 0 to 10^{-4} m/s for the water-based fluids is not a hysteresis-effect. This difference in behaviour between water and oil suggests that the water-based liquids tend to stick to the carbon-steel pipe, so that any minute amount of water introduced will start to form stagnant droplets on the walls. This picture is consistent with other experimental observations from the campaign. Specifically, it appeared that water droplets

on the wall could only be removed by flushing the system with oil and gas at the same time. Indeed, we were not able to remove the water from the wall by flushing with only gas, even at the highest gas velocity. Because of this, we regularly pre-flushed the pipe with oil and gas to avoid history-effects at low liquid rates.

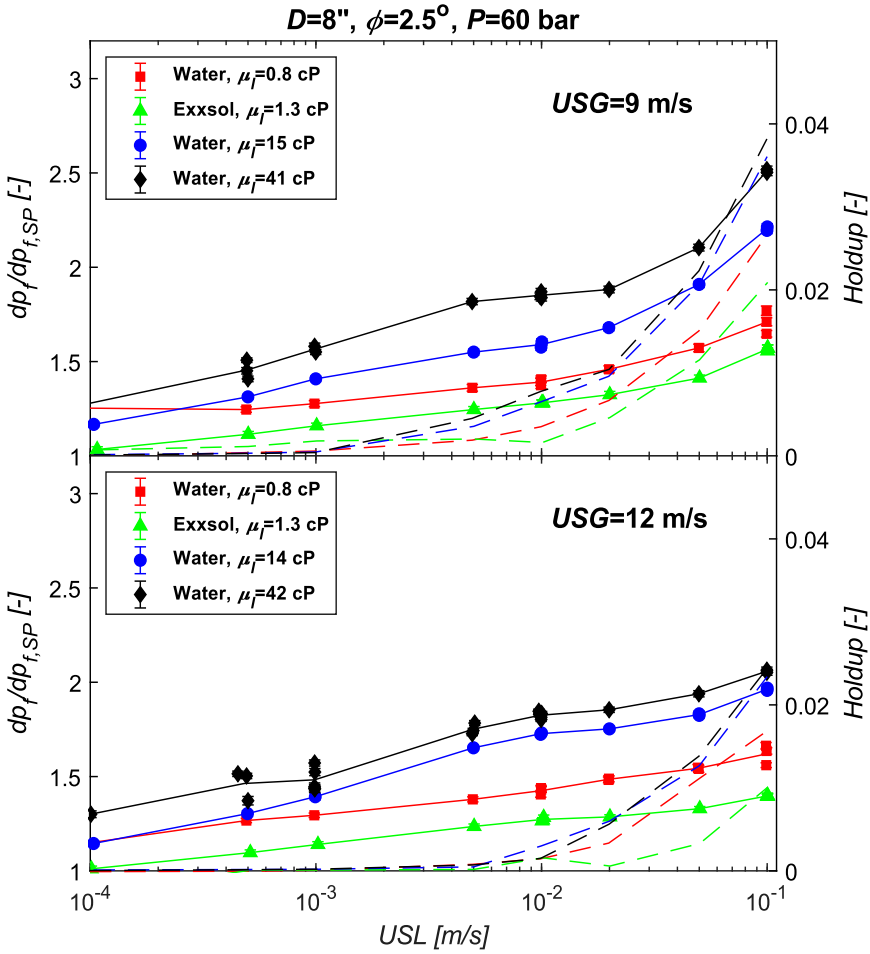

Figure 6: Normalized pressure drop (markers and solid lines) and holdup (dashed lines) plotted against *USL* for *USG*=9 and 12 m/s for the four different liquids.

4.2 Three-phase flow

Figure 7 shows results from experiments conducted in three-phase flows, where the normalized pressure drop is plotted against the water cut for *USG* = 6, 9 and 12 m/s and *USL* = 0.01 and 0.1 m/s, with the three different water viscosities.

All the plots show that the pressure drop first increases with increasing water cut, and then decreases as the water cut approaches unity. This is somewhat as expected, because we know from the oil-water experiments shown in section 3 how the oil/water mixture viscosity depends on the water cut, and we also know (from section 4.1) that the pressure drop increases with the liquid viscosity.

We observe that for all the fluid systems, the maximum pressure drop appears at a water cut around 80%. For the cases with the elevated water viscosities, this is not too surprising, since the oil-water experiments described in section 3 approximately showed that as well. However, for the case with regular water without glycerol, the oil-water experiments indicated that phase inversion occurred between 40% and 50%. It was therefore somewhat surprising that the maximum pressure drop in three-phase flows occurred at such a high water cut for this fluid system.

There may be several possible explanations for this somewhat unusual behaviour. Firstly, we must keep in mind that the local water fraction at any point within the pipe cross section may deviate significantly from the average water fraction, which we can probably assume is approximately equal to the water cut. Specifically, it is reasonable to imagine that the water fraction at the top of the pipe (within the droplet field) may be lower than the water fraction near the interface. The main reason for this would be that water droplets tend to be larger and denser than oil droplets and would thus have a more limited vertical range than oil droplets. Consequently, the water fraction in the wall film (which is formed by droplet deposition) near the top of the pipe might be lower than the average water fraction. Based on these considerations, we may conclude that the average water fraction of the wall film might be lower than the global water cut, and this would manifest itself as a right-shift of the pressure drop-versus-water cut curves. A problem with this explanation is that we only see such a shift for the regular water, and not for the water/glycerol mixture. Presumably, if this was the explanation, we would expect to see such a shift in the other fluid systems as well, so this hypothesis by itself might not be enough to explain this strange phenomenon.

Another explanation may be that the film on the wall in the gas zone does not follow the conventional "rules" of phase inversion. The experiments conducted to quantify how the viscosity varies with the water fraction are arguably only applicable to flowing situations, and not where the liquid is almost static. Video footage shows that the film on the wall moves very slowly, and may in some cases even be completely static. In such situations the kinetics of the system might be completely different from a flowing one, where the violent agitation allows the system to migrate rapidly towards the most favourable energetic state. We have observed that Exxsol and water combined with surfactants can form oil continuous emulsion layers with water fractions exceeding 90% in separators. The reason that this occurs is believed to be that the Exxsol film between the water droplets has a low mobility due to the presence of surfactants, which causes the coalescence of the water droplets to take very long. In the absence of sufficient agitation, the water droplets are able to stay intact, forming a water-dense oil-continuous emulsion. We suspect that the same phenomenon can happen to the film on the wall.

It should be noted that we did not add surfactants to the current fluid system. However, we have reason to believe that the fluid system had trace amounts of oils from previous campaigns, as well as small rust particles from the carbon steel pipe, and possibly other unknown components as well. These unknown components might affect the fluid system in a similar way as artificially added surfactants, in particular with respect to the mobility of surfaces. Indeed, it is known that surfactant concentrations of only a few parts per million can cause considerable droplet stabilization. Although this is slightly outside the scope of this paper, we may add here that we later repeated some of these three-phase experiments using a cleaner system (the flow loop was cleaned thoroughly prior to the experiments). We then found that the maximum pressure drop appeared at a water cut around 50%, and not 80%. This supports the notion that the apparent shift in inversion point shown in Figure 7 was caused by surface chemistry effects, and not hydrodynamics.

At moderate water cuts (typically ≤50%), the pressure drop appears to be more or less independent of the water properties, implying that the water properties do not play a major role in these circumstances. The reason for this is probably that the water is mostly in the form of droplets inside the oil. For higher water cuts (>50%), the pressure drop clearly increases with increasing water viscosity, suggesting that the system is no longer completely oil-continuous at those conditions.

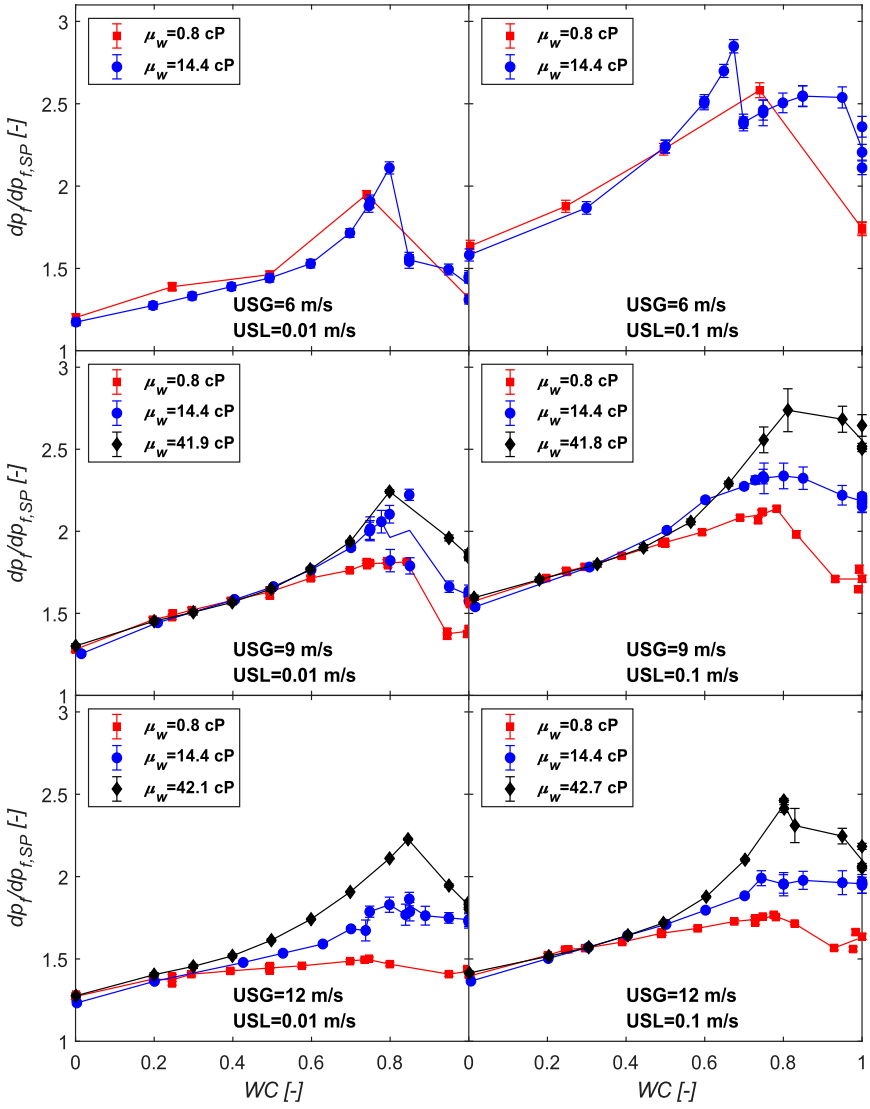

Figure 7: Normalized pressure drop plotted against the water cut for *USG*=6, 9 and 12 m/s and *USL*=0.01 and 0.1 m/s, for the three different water viscosities.

5 CONCLUSIONS

A comprehensive three-phase flow campaign was carried out in the SINTEF Large Scale Loop at Tiller. The campaign was carried out in 94 meter long 8" pipe with 2.5° inclination at 60 bar nominal system pressure.

The motivation for performing this study was to support model development targeted towards reducing prediction uncertainty for high-rate low liquid loading conditions. Specifically, the experiments were conducted at conditions that to a certain extent match those expected during plateau production for the subsea gas development in Block 2 offshore Tanzania [1]. One of the key concerns was that the presence of oil and water increases the frictional pressure drop more than current multiphase models predict.

The focus of the work was on gas dominated three-phase flows, with low liquid rates (*USL*=0.00001-0.1 m/s), and mainly high gas rates. The superficial gas velocities were *USG*=4-14 m/s and the water cut was varied from 0% to 100%.

The effect of the water viscosity was investigated by mixing glycerol (70-74%) with the water and conducting experiments at different temperatures. The motivation for investigating the water viscosity was that MEG will be used for hydrate prevention in the Tanzania field, which can increase the water viscosity significantly. The temperatures used were in the range 23-45°C, yielding viscosities in the range 14-42 cP.

The aim of the experimental campaign was to produce experimental data relevant for modelling two- and three-phase low liquid loading flows at high gas rates. Earlier experiments [2] had revealed that the pressure drop was significantly higher in three-phase flows compared to two-phase flows, and the current experiments were conducted to investigate this phenomenon more thoroughly.

The most important findings from the experiments were:

- For low *USL* (*USL*=0.01 m/s), the normalized pressure drop increases with *USG* for "moderate" *USG*, and then reaches a maximum after which the normalized pressure drop decreases. At higher *USL* (*USL*=0.1 m/s), the normalized pressure drop decreases more or less monotonously with *USG*.
- For the flow conditions explored here, the pressure drop in gas/tap-water experiments are greater than in the respective gas/oil experiments, despite the fact that the oil viscosity is higher than the water viscosity. The typical difference is around 10%. This systematic difference may be related to the higher value of surface tension for the water.
- For the gas/water experiments, the pressure drop and liquid holdup increases with increasing liquid viscosity.
- The pressure drop increases with increasing *USL*. For very low *USL* (10^{-4} m/s), the pressure drop in the gas-oil system is approximately equal to the pressure drop in single phase gas, while for the associated gas-water systems, the pressure drop is typically 10-30% higher, depending on the gas flow rate and water viscosity.
- The pressure drop depends significantly on the water cut. In general, the pressure drop increases with water cut, reaching a maximum value at around *WC*=80%, after which the pressure drop decreases until the value for gas-water is obtained. This is the case for all three water viscosities, although the maximum pressure drop clearly increases with increasing water viscosity.

- At moderate water cuts (typically ≤50%), the pressure drop is more or less independent of the water properties, implying that the water properties do not play a major role in these circumstances. The reason for this is probably that the water is mostly in the form of droplets inside the oil. For higher water cuts (>50%), the pressure drop clearly increases with increasing water viscosity, suggesting that the system is no longer completely oil-continuous at those conditions.

6 ACKNOWLEDGEMENTS

The authors would like to express their gratitude to the technical and scientific personnel at Tiller for their considerable efforts during the experimental campaigns. Also, we wish to thank Equinor and the Tanzania Gas Development Project - Block 2 for their financial support of these experiments, and for their approval of this publication.

7 REFERENCES

[1] H. Holm, "Tanzania gas development - flow assurance challenges," in *BHRG*, Cannes, 2015.

[2] H. Holm, "Tanzania Flow Assurance Challenges updated," in *BHRG*, Cannes, 2017.

[3] H. Holm, "Tanzania Flow Assurance Challenges (Equinor ASA)," in *BHRG*, Cannes, 2019.

[4] J. Kjølaas, T. E. Unander, M. Wolden, A. Shmueli and H. Holm, "Pressure drop measurements in low liquid loading three-phase flows," in *17th International Conference on Multiphase Production Technology*, Cannes, 2017.

[5] D. Biberg, C. Lawrence and G. Staff, "Pressure drop in low liquid loading flows - the effect of a thin liquid film on the pipe wall," in *BHRG*, Cannes, France, 2017.

[6] R. Pal and E. Rhodes, "Viscosity/Concentration Relationships for Emulsions," *Journal of Rheology*, vol. 33, no. 7, 1989.

[7] H. Schümann, J. Kjølaas, M. Wolden, C. Lawrence and H. Holm, "Rheology study: Comparison of a real condensate-MEG system and a model fluid system used in the Tiller Low-Liquid-Loading campaigns," in *18th International Conference on Multiphase Production Technology*, Cannes, 2019.

[8] G. Chupin, "An Experimental Investigation of Multiphase Gas-Liquid Pipe Flow at Low Liquid Loading," NTNU, Trondheim, 2003.

[9] H. Karami, C. F. Torres, E. Pereyra and C. Sarica, "Experimental Investigation of Three-Phase Low-Liquid-Loading Flow," in *SPE Annual Technical Conference and Exhibition*, Houston, 2016.

[10] H. K. Dong, "Low Liquid Loading Gas-Oil-Water Flow in Horizontal Pipes- MS Thesis," The university of Tulsa, Tulsa, Oklahoma, 2007.

[11] G. F. Hewitt, "Three-phase gas–liquid–liquid flows in the steady and transient states," *Nuclear Engineering and Design*, vol. 235(10–12), pp. 1303-1316, 2005.

[12] Emerson. [Online]. Available: http://www.emerson.com/en-us/automation/micro-motion.

[13] "National Institute of Standards and Technology," [Online]. Available: http://webbook.nist.gov/chemistry/fluid/.

[14] S. Håland, “Simple and Explicit Formulas for the Friction Factor in Turbulent Flow,” *Journal of Fluids Engineering (ASME)*, vol. 105, no. 1, pp. 89-90, 1983.

[15] H. Brinkman, “The viscosity of concentrated suspensions and solutions,” *J. Chem. Phys.*, vol. 20, no. 4, pp. 571-584, 1952.

[16] J. Kjølaas, “Modelling of the wall film in high-rate low liquid loading flows,” in *18th International Conference on Multiphase Production Technology*, Cannes, 2019.